

## SIMPLE METHOD TO ENHANCE CT BRAIN IMAGES FOR USE IN DIAGNOSIS OF ACUTE CEREBRAL ARTERY INFARCTION

*Du-Yih Tsai*<sup>1</sup>, *Noriyuki Takahashi*<sup>2</sup>, *Yongbum Lee*<sup>1</sup>, and *Katsuyuki Kojima*<sup>3</sup>

<sup>1</sup> Department of Radiological Technology, School of Health Sciences, Niigata University, Niigata-city, Niigata, 951-8518, Japan. (tsai@clg.niigata-u.ac.jp; lee@clg.niigata-u.ac.jp)

<sup>2</sup> Department of Radiology, Sendai City Hospital, 3-1 Shimizu-koji, Wakabayashi-ku, Sendai-city, Miyagi, 984-0075, Japan. (norizaemon@pop02.odn.ne.jp)

<sup>3</sup> Department of Information Networks, Faculty of Administration and Informatics, University of Hamamatsu, 1230, Miyakodacho, Hamamatsu-shi, Shizuoka, 431-2102, Japan. (kojima@hamamatsu-u.ac.jp)

**Abstract:** In this paper we propose a simple method aiming at improving the visibility of the loss of the gray-white matter interface in computer tomography (CT) brain images. The loss of the gray-white matter interface is one of the early signs of acute cerebral artery infarction (ACAI). The method is to employ our proposed adaptive smoothing filter (ASF) to reduce local noise with edges preserved in CT brain images. The ASF is a specially designed filter with adaptive size and shape depending on local pixel-value-related information surrounding the pixel of interest. In order to demonstrate the superiority of the ASF, two commonly used filters for image smoothing, *i.e.*, the averaging filter and the median filter were used for comparison. Two criteria, standard deviation and slope ratio, were adopted in this study for performance assessment. Moreover, the ASF was also applied to clinical CT brain images in hyperacute stroke patients for performance evaluation. Our preliminary results showed that the detectability of early infarct signs is much improved. The results demonstrate the superiority of the proposed method and its usefulness.

**Keywords:** medical image processing, adaptive image filtering, feature measurement.

### 1. INTRODUCTION

Currently computed tomography (CT) is widely accepted as the imaging modality for acute cerebral artery infarction (ACAI) investigation. The loss of gray-white matter interface is one of the early signs of ACAI [1-3]. However, in most cases, the subtle appearance of the loss of gray-white matter interface resulting from quantum noise can not be visually identified by the clinicians. Therefore image processing for image enhancement is required. However, conventional enhancement algorithms reduce image noise at the expense of blurring of lines and edges of the image. So far, some techniques, such as adaptive Wiener filters [4, 5] and anisotropic adaptive filtering [6, 7] have been proposed. Nevertheless, most of these adaptive filters are useful for specific applications. Further, these techniques are extreme time consuming resulting in precluding their use in real-time application.

As far as we know, until now, no work has focused on improving the visibility of normal gray-white matter interface on CT brain images by using a noise reduction filter. Noise reduction with conventional smoothing filters generally accompanies blurring of edge. This causes the blurring of the normal gray-white matter interface on CT images.

In the present study we propose an adaptive smoothing filter (ASF) aiming at improving the visibility and detectability of the loss of the gray-white matter interface. The proposed technique can enhance image data by removing noise without significantly blurring the structures in the CT image. The advantage of this approach is its simplicity of processing, which in turn reduces computation time. To validate the clinical effectiveness of the proposed method, CT images with the ACAI were used for evaluation.

### 2. METHODS AND MATERIALS

Our proposed ASF is a specially designed filter used to perform local smoothing using a variable filter size and shape. The approach to thresholding employed in the ASF partly refers to a report related to adaptive neighborhood contrast enhancement [8]. Fig. 1 shows the flow chart of the technique's main steps and they are as follows.

(1) After applying a  $5 \times 5$  averaging filter to the original image, each pixel  $(i,j)$  of the image  $I$  is assigned an upper window  $W_{\max}$  centered on it whose size is smaller than the original image, where  $W_{\max}$  is an odd number.

(2) Let  $T$  be a given threshold. Pixel  $(k,l)$  within  $W_{\max}$  is assigned a binary mask value 0 if  $|I(k,l) - I(i,j)| > T$ , else it is assigned a binary mask value 1. This results in constructing a binary image. Fig. 2 shows an example in the case of  $T=5$  and  $W_{\max}=9$ .

(3) For each window size  $C \times C$  [ $C=3,5,\dots, W_{\max}$ ], the percentage  $P_0$  of zeros is computed over the region of external area of  $C \times C$  window. This computation process stops if  $P_0 > 60\%$ . Let  $C_0$  be the upper  $C$  value beyond which the percentage  $P_0$  is greater than 60%. Then the pixel  $(i,j)$  is assigned the window having a size of  $W = C_0 \times C_0$ . The value of 60% was chosen because beyond this limit, we may con-

sider too many 0 pixels are surrounding the inner area and so the notion of neighborhood with the central pixel (i,j) in terms of gray levels is no longer satisfactory [8].

(4) Finally, the processed image  $I'$  is obtained from  $I'(i, j) = M(i, j)$ , where  $M(i, j)$  is the mean value in image  $I$  of pixels labeled as the binary mask value 1 in the window  $C_0 \times C_0$  around pixel (i, j).

However, it is noted that the quality of the processed image depends on the threshold value  $T$ . Determination of optimal threshold value is, therefore, required to make the ASF having best performed. To this end, the standard deviation and slope ratio of the image are used as two criteria for measuring the performance of the ASF. To conduct the measurement of the performance, ten composite images as shown in Fig.3 were generated by adding a computer-simulated gray matter to each uniform phantom image obtained from a 4-slice CT scanner.

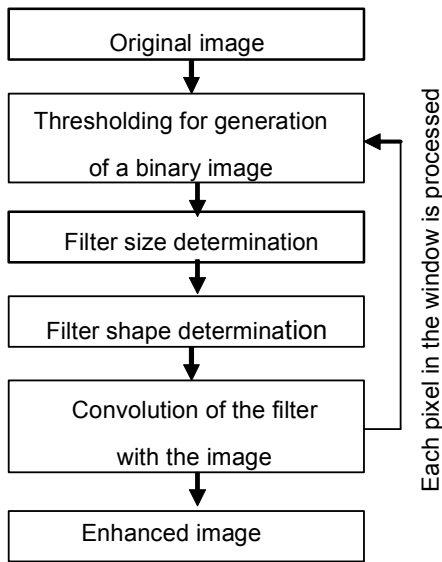


Fig. 1. Flow chart of the main steps of the proposed image-processing technique.

31	36	41	43	45	45	45	36	46
32	35	35	35	36	36	34	35	45
31	36	36	33	34	33	35	50	45
29	35	35	36	<b>33</b>	34	50	50	50
25	34	34	35	<b>35</b>	34	50	51	51
32	35	33	32	34	33	51	35	50
39	25	34	35	34	45	46	45	45
25	24	25	32	20	20	21	20	43
24	25	31	32	32	20	45	43	41

1	1	0	0	0	0	0	1	0
1	1	1	1	1	1	1	1	0
1	1	1	1	1	1	1	0	0
0	1	1	1	<b>1</b>	1	0	0	0
0	1	1	1	1	1	0	0	0
1	1	1	1	1	1	0	1	0
1	0	1	1	1	0	0	0	0
0	0	0	1	0	0	0	0	0
0	0	1	1	1	0	0	0	0

Fig. 2. Adaptive neighborhood selection with a threshold value  $T=5$ . Pixel (k,l) within  $W_{max}$  is assigned a binary mask value 0 if  $|I(k,l) - I(i,j)| > T$ , else it is assigned a binary mask value 1. (a)  $W_{max}$  window around bold-faced pixel value 35; (b) mask values associated to test pattern in (a).

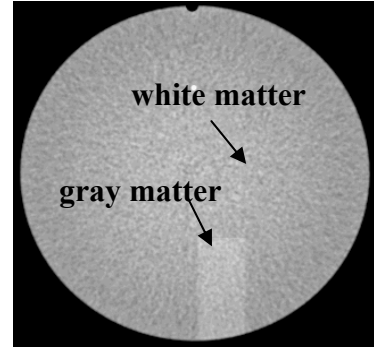


Fig.3. A computer-simulated composite image.

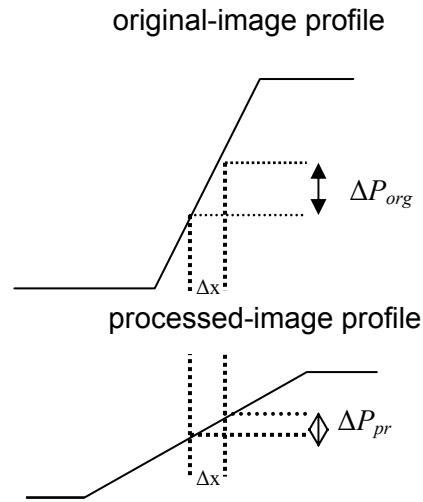


Fig. 4. Slope ratio is defined as the ratio of the profile slope of the processed image ( $\Delta P_{pr} / \Delta x$ ) to that of the original image ( $\Delta P_{org} / \Delta x$ ).

In this study, the standard deviation (SD) of the pixel values in a specified area, which is used to quantify the degree of noise reduction, was obtained from a region of interest in the composite images. Low standard-deviation value means that high reduction of noise can be obtained by the ASF.

To investigate the extent of edge blurring, slope ratio was calculated from a profile of pixel values, which was measured at the right angle with respect to the edge of gray-white matter. In this work, the slope ratio (SR) is defined as the ratio of the profile slope of the processed image to that of the original image, and can be given as

$$SR(\%) = (\Delta P_{pr} / \Delta x) / (\Delta P_{org} / \Delta x) \times 100, \quad (1)$$

where  $(\Delta P_{pr} / \Delta x)$  and  $(\Delta P_{org} / \Delta x)$  are the profile slope of the processed image and that of the original image, respectively (Fig.4). Low slope-ratio value means that high edge blurring occurs resulting from the ASF.

### 3. RESULTS AND DISCUSSION

The effect of threshold-value determination on the standard deviation of the composite images was calculated and the results are shown in Fig. 5. It is noted that the standard-deviation value decreases with the increase of threshold value and maintains constant when the threshold value is higher than 3.0. Therefore, noise reduction can be effectively achieved if the threshold value is set at  $T=3.0$ . In this case, the standard-deviation value of the original image is 2.5 and that of the processed image is 0.6. As a result, a 76% of the noise reduction can be obtained.

The variation of the slope ratio with the threshold value used in the ASF for the composite image was also investigated and the results are shown in Fig. 6. The slope ratio is at approximately 60% for the threshold values ranging from 0 to 3.0 and gradually declines when the threshold value is greater than 3.0. Recall that low slope-ratio value shows high edge blurring. Therefore, the edge blurring of the composite image can be suppressed if the threshold value is set at 3.0 or less. From the two experimental results, it is reasonable to conclude that  $T=3.0$  is the optimal value used in the ASF for image improvement in noise reduction.

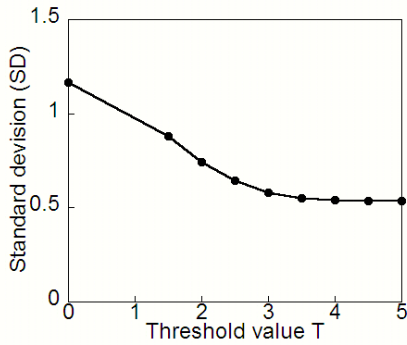


Fig. 5. A plot of the standard deviations computed by varying the threshold value  $T$ .

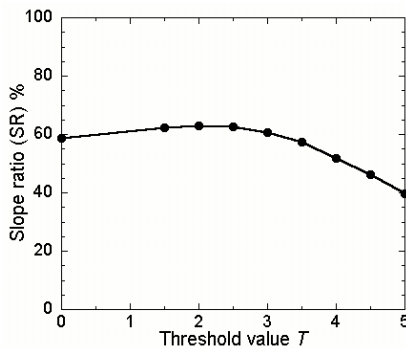


Fig. 6. A plot of the slope ratios computed by varying the threshold value  $T$ .

In order to demonstrate the superiority of the ASF, we also applied two commonly used smoothing filters, *i.e.*, the averaging filter and the median filter, to the composite images for comparison. The SD and SR were used for performance assessment. We tried to keep the value of SDs at nearly the same and then to compare the values of SR which is considered as an index for expressing the edge blurring of the images caused by image processing. The results are summarized in Table 1. The results indicate that the performance of the proposed method is superior to the other two filters. Fig. 7 shows the results obtained by applying the three methods to the same composite image. It is visually evident that the ASF significantly enhances the image as compared to the averaging and median filters. The ASF with the pre-determined optimal condition of thresholding  $T=3.0$  was applied to two un-enhanced CT images obtained at 2 ½ hours after stroke onset. Figs. 8 and 9 illustrate our experimental results. The two cases had been diagnosed as normal when reading the original images in the first CT scans. After executing image processing on the original images by using the ASF, the loss of gray-white matter interface in the lentiform nucleus and/or the cortical ribbon, *i.e.*, the early sign of the ACAI, could be clearly detected. Fig.8(c) shows the follow-up non-enhanced CT image obtained four days after ictus demonstrates ACAI (Arrows). Fig. 9(c) shows the MR image obtained immediately after the CT examination. Our results showed that the visibility and detectability of the loss of gray-white matter interface were much improved by the proposed method.

However, the number of patients included was limited. To solve this issue, we are currently working on the examination of the sensitivity of our proposed method in detection of the ACAI with a larger data set.

Table 1. Slope ratios evaluated on the composite images after applying the ASF, averaging filter and median filter.

Filter	Standard Deviation	Slope Ratio (%)
ASF	0.59	59.9
Averaging	0.60	21.3
Median	0.61	31.2

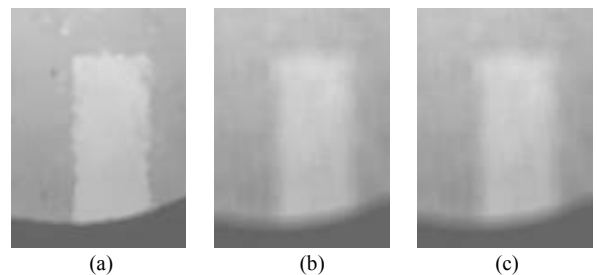


Fig. 7. Results obtained from the composite image after applying (a) the ASF, (b) the averaging filter, and (c) the median filter.

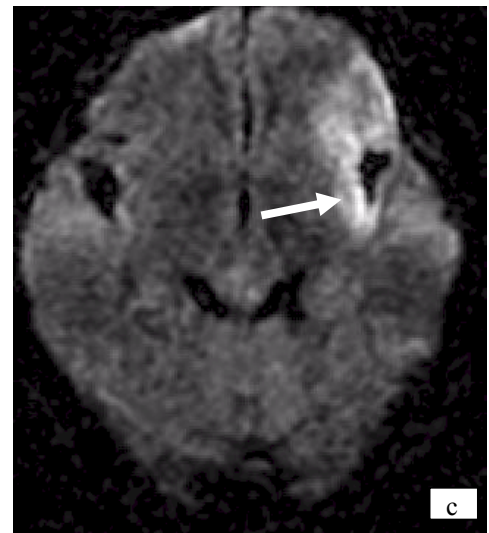
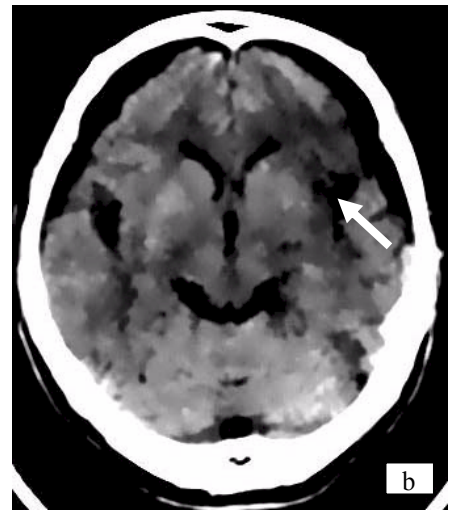
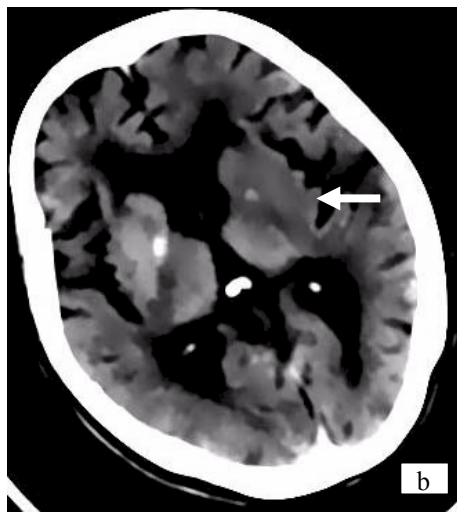
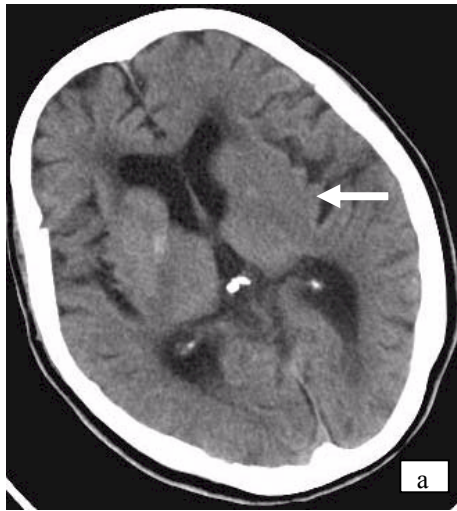


Fig. 8. CT image from a 83-year-old female with right hemiplegia at 2 ½ hours after stroke onset. (a) original image, (b) processed image and (c) follow-up CT image taken four days after stroke onset.

Fig. 9. CT image from a 67-year-old male with right hemiplegia at 2 ½ hours after stroke onset. (a) original image, (b) processed image and (c) follow-up MR image taken immediately after the CT scan.

#### 4. CONCLUSION

In this study we have proposed an adaptive smoothing filter aiming at improving the visibility and detectability of the loss of gray-white matter, which is considered as one of the important early signs of ACAI. In order to obtain the optimal thresholding value used in our proposed filter, we have measured the standard deviation and slope ratio of the image of interest, which are respectively used to describe the degree of noise reduction and that of edge blurring of the images enhanced by the proposed method. Our results have demonstrated that the visibility and detectability of the loss of gray-white matter interface have been much improved by the presented method. The results also showed that the proposed ASF performed well and clinically useful. In particular our proposed method could be a strong strategy for determining eligibility for thrombolytic therapy in ischemic stroke.

#### ACKNOWLEDGMENTS

The authors would like to thank Kiyoshi Ishii, MD, of Sendai City Hospital for his contribution to this study. This work is supported in part by the Telecommunication of Advancement Foundation, Japan.

#### REFERENCES

- [1] U. Tamura, K. Uemura, A. Inugami, H. Fujita, S. Higano, F. Shishido, "Early CT finding in cerebral infarction: obscuration of the lentiform nucleus", *Radiology*, Vol. 168, pp. 463-467, 1988.
- [2] T. Moulin, F. Cattin, T. Crepin-Leblond, L. Tatu, D. Chavot, M. Piotin, et al, "Early CT signs in acute middle cerebral artery infarction: predictive value for subsequent infarct locations and outcome", *Neurology*, Vol. 47, pp. 366-375, 1996.
- [3] H. P. Jr Adams, R. J. Adams, T. Brott, G. J. del Zoppo, A. Furlan, L. B. Goldstein, et al, "Guidelines for the early management of patients with ischemic stroke: a scientific statement from the Stroke Council of the American Stroke Association", *Stroke*, Vol. 34, pp. 1056-1083, 2003.
- [4] X. You and G. Crebbin, "A robust adaptive estimator for filtering noise in images", *IEEE Transactions on Image Processing*, Vol. 4, No. 5, pp. 693-699, 1995.
- [5] J. A. S. Centeno and V. Haertel, "An adaptive image enhancement algorithm", *Pattern Recognition*, Vol. 30, No. 7, pp. 1183-1189, 1997.
- [6] B. Fischi and E. Schwartz, "Adaptive non-local filtering: a fast alternative to anisotropic diffusion for image filtering", *IEEE Transaction on Pattern Analysis and Machine Intelligence*, Vol. 21, No. 1, pp. 42-48, 1999.
- [7] C.-F. Westin, J. Richolt, V. Moharir and R. Kikinis, "Affine Adaptive of CT data", *Medical Image Analysis*, Vol. 4, No. 2, 161-177, 2000.
- [8] V.H. Guis, M. Adel, M. Rasigni, G. Rasigni, B. Seradour, and P. Heid, "Adaptive neighborhood contrast enhancement in mammographic phantom images", *Opt. Eng.*, Vol. 42, No. 2, pp. 357-366, 2003.